Innovative Infrastructure Solutions (2018) 3:15
https://doi.org/10.1007/s41062-017-0121-4

SHORT COMMUNICATION

Finite element evaluation of ultimate capacity of strip footing: assessment using various constitutive models and sensitivity analysis

Jitesh T. Chavda[1] · **G. R. Dodagoudar**[1]

Received: 9 October 2017 / Accepted: 25 December 2017 / Published online: 10 January 2018

Abstract
Finite element method can be used for computing bearing capacity of shallow foundation with irregular geometry resting on variable subsoil. It is necessary to quantify the parameters affecting the ultimate capacity of footing. This paper presents the results of finite element (FE) analysis of the ultimate failure load of a rough base rigid strip footing resting on c-ϕ soil. The soil is assumed as linear elastic perfectly plastic with Mohr–Coulomb failure criterion and non-associative flow rule. Sensitivity analysis is carried out to examine the ultimate capacity of strip footing considering the strength parameters (c', ϕ', and ψ), width of strip footing (B), unit weight of soil (γ), surcharge (q) at the base level of footing, and the deformation parameters (E and ν) as the variables. The study also examines the effect of different material models on the ultimate capacity of the strip footing. The material models considered are Mohr–Coulomb (MC) model, Hardening Soil (HS) model, Hardening Soil model with small-strain stiffness (HSsmall), and Soft Soil (SS) mode-l. It is found from the results of FE analysis that the ultimate load of the strip footing is dependent on the strength parameters, width of footing, unit weight of soil, and surcharge at the base level of the footing. The ultimate capacity is independent of the deformation parameters and will remain almost same corresponding to the material models like MC, HS, HSsmall, and SS. The FE results are compared with the analytical solutions of Terzaghi and Meyerhof. Based on the study, a few suggestions are given in regard to the FE analysis of geotechnical stability problems to obtain the quick results.

Keywords Strip footing · c-ϕ soil · Material model · Ultimate load · Finite element method · Sensitivity analysis · Triaxial test

Introduction

The goal of numerical modeling in geotechnical engineering is to understand the behavior of geotechnical structures, evaluation of soil displacements and footing deflection under applied loads, calculation of internal forces like shear, axial, torsion and bending moment necessary for the design of structural elements, and to predict the possible failure mechanisms. In computational geomechanics, advanced constitutive models are being used to determine the realistic soil displacements and structural deformations under working loads, to check the serviceability (settlement of footing within the allowable limits), and to determine the ultimate load and corresponding failure mechanism.

The ultimate load which causes the failure of a footing is needed to determine the ultimate bearing capacity of the footing. The estimation of bearing capacity of a shallow foundation is a vital task in the design of low-rise structures. The solution to the bearing capacity of strip footing is determined by utilizing the limit equilibrium methods [11, 19, 26], method of stress characteristics [1, 14, 28], upper and lower bound limit analyses [3, 6, 7, 15, 16, 20, 22, 24, 25, 27], limit analysis [5, 13, 21], finite element method (FEM) [4, 9, 10, 12, 31], and finite difference method [17, 29]. In numerical analysis, the material failure criteria have to be defined for stability analysis of the geotechnical systems. Most of the above-mentioned analyses use Mohr–Coulomb model. It is noted that the solutions obtained for the given

✉ Jitesh T. Chavda
jiteshchavda03@yahoo.in

G. R. Dodagoudar
goudar@iitm.ac.in

[1] Computational Geomechanics Laboratory, Geotechnical Engineering Division, Department of Civil Engineering, Indian Institute of Technology Madras, Chennai 600036, India

type of problem are corresponding to the material model used in the analysis.

Need of the study

The Mohr–Coulomb model is most widely used constitutive model in the numerical simulation of soil behavior. Of late, a few advanced constitutive models have been utilized in the stability analysis of geotechnical structures. If the aim of the analysis is to determine the ultimate limit state, the failure load obtained from the finite element (FE) analysis is corresponding to the defined strength parameters. This means, the applicability of the model being used depends on the results of interest. If the deformations, stresses, displacements, forces in the members, etc., are needed to be evaluated at the working load, the constitutive model used in the analysis plays a vital role. However, for the determination of ultimate failure load, the assigned model whose failure envelope is based on the Mohr–Coulomb failure criterion will give more or less the same failure load at the ultimate limit state. Moreover, the material model to be used in the numerical analysis should comply with the requirements of the aim of the analysis. Hence, there is a need to quantify the dependency of the parameters affecting the failure load (i.e., collapse load) and to select the suitable material models for the determination of ultimate failure load.

In this study, the FE sensitivity analysis is carried out to quantify the dependency of the parameters, which are used in the Mohr–Coulomb material model, on the ultimate failure load of the strip footing. The ultimate failure loads are also calculated using other advanced material models like HS, HSsmall, and SS. A triaxial test is simulated using the FE analysis to determine the effect of these models on the assessment of failure stress and stress paths. The results of the parametric studies are compared with the classical solutions of the strip footing given by Terzaghi [26] and Meyerhof [19].

Problem definition

The ultimate bearing capacity of a shallow foundation is usually calculated using the classical solution of Terzaghi [26]. The equation is expressed as

$$\frac{Q_{\mathrm{u}}}{B} = q_{\mathrm{u}} = cN_c + qN_q + \frac{1}{2}\gamma BN_\gamma \tag{1}$$

where Q_{u} is the ultimate failure load, q_{u} is the ultimate bearing capacity of soil, c is the soil cohesion, q is the surcharge at the base level of the footing, γ is the unit weight of soil, B is the width of footing and N_c, N_q, and N_γ are the bearing capacity factors which account the effect of soil cohesion, surcharge, and unit weight of soil, respectively. The bearing capacity factors are function of the friction angle of the soil. Equation (1) is based on the principle of superposition of the effects of soil cohesion, surcharge, and unit weight of the soil. Based on this equation, the ultimate failure load (Q_{u}) depends on the soil cohesion (c), surcharge (q), unit weight of the soil (γ), the width of footing (B), and the friction angle of the soil (ϕ). The dilatancy angle of soil (ψ) is not considered in Eq. (1). The FE analysis is carried out to determine the collapse load of the strip footing by varying the above-mentioned parameters. In the FE analysis, in order to compute the collapse load, the deformation parameters (E and ν) are also required. Thus the study also examines the effect of varying E and ν on the collapse load of the footing.

Finite element analysis

The FE analysis is performed to compute the failure load of rough base strip footing using PLAXIS-2D-Version 2016.01 program. The PLAXIS is a user-friendly software developed exclusively for the analysis of geotechnical systems.

Soil constitutive relation and boundary conditions

In the study, the soil is assumed as homogeneous and isotropic with linear elastic perfectly plastic behavior and obeys the non-associated flow rule. The Mohr–Coulomb model is assigned to the FE model of the strip footing. The material properties assigned to the soil elements are given in Table 1. The FE mesh, boundary conditions, and model dimensions are depicted in Fig. 1 based on the convergence study. PLAXIS provides 6- and 15-node triangular elements only for the modeling of soil continuum elements. For higher accuracy, 15-node triangular elements with 12 Gaussian quadrature points are used in the analyses. The meshing selected for the FE model in PLAXIS is the fine mesh. The boundary conditions are assigned as roller supports at the sides to allow the movement only in the vertical direction and the lower boundary is fixed in both the directions (Fig. 1). The FE mesh dimensions are changed and the formation of plastic regions is checked. The overall FE mesh dimensions have been finalized based on the formation of plastic regions, which are contained well within the FE domain. The FE mesh dimensions for strip footing are obtained as 30 m in the horizontal direction and 15 m in the vertical direction. The groundwater table is not considered in the analysis.

Table 1 Input parameters of the material models used in the FE analysis

Parameters	Symbol	Units	Material model			
			MC	HS	HSsmall	SS
Unit weight	γ	kN/m^3	20	20	20	20
Cohesion	c'	kPa	10	10	10	10
Friction angle	ϕ'	Degree	10	10	10	10
Dilatancy angle	ψ'	Degree	0	0	0	0
Young's modulus	E	MPa	100	–	–	–
Poisson's ratio	ν	–	0.35	0.2	0.2	0.2
Secant stiffness	E_{50}	MPa	–	50	50	–
Tangent stiffness	E_{oed}	MPa	–	48	48	–
Unloading/reloading stiffness	E_{ur}	MPa	–	102	102	–
Power for stress level dependency of stiffness	m	–	–	0.5	0.5	–
Coefficient of earth pressure at rest	K_0	–	0.826	0.826	0.826	0.826
K_0-value for normal consolidation	K_0^{nc}	–	–	0.75	0.75	0.7265
Failure ratio	R_f	–	–	0.9	0.9	–
Maximum shear modulus	G_0^{ref}	MPa	–	–	100	–
Shear strain	$\gamma_{0.7}$	–	–	–	0.001	–
Modified compression index	λ^*	–	–	–	–	0.003
Modified swelling index	κ^*	–	–	–	–	0.0019

MC Mohr–Coulomb model, *HS* Hardening Soil model, *HSsmall* Hardening Soil model with small-strain stiffness, *SS* Soft Soil mode-l

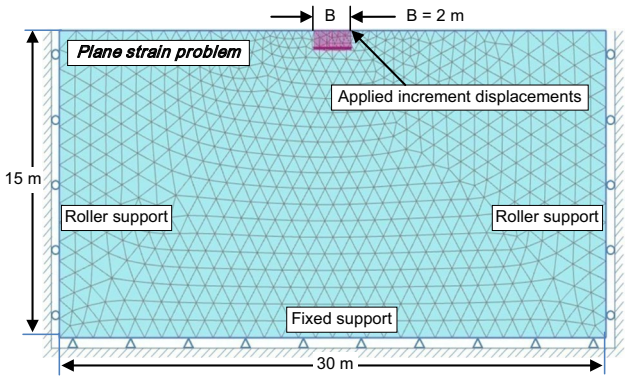

Fig. 1 FE mesh, boundary conditions and model dimensions

Footing roughness and determination of ultimate load

The footing roughness has a major effect on the unit weight component of Eq. (1) and very less effect on the soil cohesion and surcharge [1, 9, 18, 19]. In the present study, the footing is modeled as rigid footing with rough base in order to compare the results obtained from FE analysis with the solutions of rigid and rough strip footings considered by Terzaghi [26] and Meyerhof [19]. In the case of rough base footing, the nodes representing the footing width are restrained in the horizontal direction. The rigid behavior of the rough base strip footing is accounted by applying the increment displacements (prescribed displacements) at the nodes representing the footing width in the FE analysis. The total prescribed displacement of 500 mm is assigned. The prescribed displacements may start from smaller values; however, in this case, it is difficult to obtain the ultimate load. In the FE analysis, the prescribed displacement is selected little higher than the displacement at which the ultimate load is expected. The analysis is stopped when the load reached the ultimate state of stress, i.e., the displacement of the footing keeps on increasing and corresponding load remains constant. At this point, the soil zone contributing to the ultimate load of the footing is reached to its full plastic state thereby mobilizing its shear strength [9]. The load vs. displacement is then plotted to determine the value of ultimate failure load. This failure load is the ultimate one and will remain constant thereafter.

Sensitivity analysis

As per Terzaghi's classical solution of strip footing [Eq. (1)], the ultimate bearing capacity of soil is directly proportional to the friction angle of soil, soil cohesion, unit weight of soil, the surcharge at the base of footing, and the width of footing. The parametric sensitivity analyses are carried out to determine the ultimate failure load of the strip footing with varying parameters of the Mohr–Coulomb model to quantify the effect of these parameters on the ultimate capacity of the strip footing. The following parameters are used in the basic FE model of the strip footing: strength parameters ($c' = 10$ kPa, $\phi' = 10°$, and $\psi = 0°$), unit weight of soil

($\gamma = 20$ kN/m^3), surcharge ($q = 0$ kPa), and deformation parameters ($E = 100$ MPa and $\nu = 0.35$). The width of footing (B) is taken as 2 m.

The effect of soil cohesion on the ultimate capacity of the strip footing is studied by computing the ultimate load corresponding to the variation in the value of cohesion as $c' = 5$, 10, and 15 kPa and keeping the other parameters as constant in the basic FE model of the strip footing. Similarly, the effect of other parameters on the ultimate capacity of the strip footing is studied by varying the friction angle of the soil ($\phi' = 5$, 10, and 15°), width of the footing ($B = 1$, 2, and 3 m), unit weight of soil ($\gamma = 5$, 10, and 15 kN/m^3), and surcharge ($q = 0$, 25, and 50 kPa). It is noted that the smaller values of unit weight of soil are chosen in order to highlight the efficacy of the FEM. It is noted that the Terzaghi's bearing capacity equation of the strip footing is independent of the deformation parameters E and ν. In order to quantify the effect of Young's modulus and Poisson's ratio of the soil, in the basic FE model of the strip footing, the values of E and ν are varied as $E = 50$, 100, and 200 MPa and $\nu = 0.15$, 0.25, 0.35, and 0.45 and the corresponding ultimate loads are computed.

The usage of material models in the FE analysis depends on the type of soil, response of the soil to be captured, and type of the loading. To quantify the effect of different material models on the ultimate capacity of the strip footing, the four material models, viz. Mohr–Coulomb (MC) model, Hardening Soil (HS) model, Hardening Soil model with small-strain stiffness (HSsmall), and Soft Soil (SS) model are used in the FE analysis. The input parameters corresponding to each of these models (MC, HS, HSsmall, and SS) are given in Table 1. A brief description of the above-mentioned material models is given in Appendix 1.

Results and discussion

Strip footing

Ziccarelli et al. [30] have carried out centrifuge experiments on model strip footing of width $B_m = 40$ mm at 25-g. The prototype width of the strip footing was $B_p = 1$ m. The overall dimensions of the model tank are length = 0.62 m, height = 0.28 m, and width = 0.16 m. The FE model shown in Fig. 1 is selected for the validation. In FE model, the same material parameters as used in the centrifuge experiment are assigned. They are: $\gamma = 16.1$ kN/m^3, $\phi = 47.8°$, $\psi = 19.5°$, $E = 125$ MPa, and $\nu = 0.15$. It is to be noted that a negligible value of cohesion is assigned (i.e., $c = 1$ kPa) in the analysis as recommended by Brinkgreve et al. [2]. The Mohr–Coulomb material model and non-associative flow rule are used in the FE model. The FE and experimental results are compared in Fig. 2a. The discrepancy in the FE results of the order of 7% is noted in comparison with the experimental results. The small instability of numerical results in the pre-peak phase is observed and that is due to the non-associativity of the constitutive model [8]. Parametric sensitivity analysis with respect to Young's modulus ($E = 75$, 100, and 125 MPa) is performed to compare the centrifuge results with that of the FE results. Figure 2b depicts the effect of Young's modulus on the ultimate failure load of the strip footing. It can be observed from the figure that the ultimate failure load of the footing is remains almost the same with the varying values of the Young's modulus of the soil. Based on the comparison (Fig. 2a, b), it is noted that the FE results are agreeing reasonably well with the centrifuge experiment.

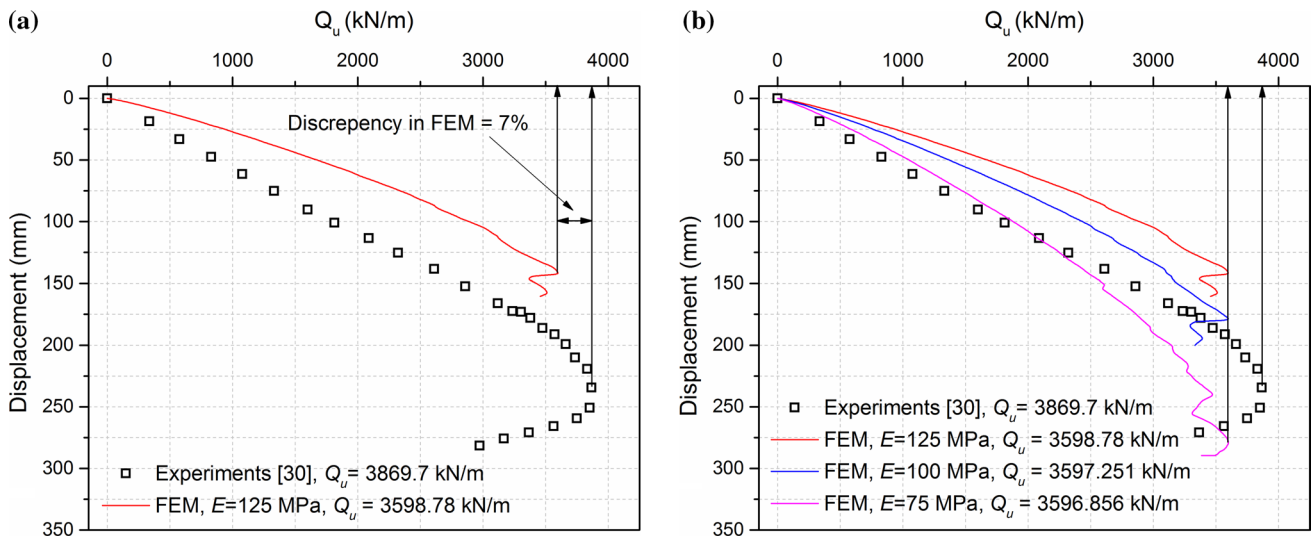

Fig. 2 Load vs. displacement plot of strip footing: **a** comparison of FE and centrifuge results, **b** comparison with varying Young's modulus

Effect of strength parameters of soil

The effect of soil cohesion on the ultimate capacity of the strip footing is depicted in Fig. 3a. It is observed from the load vs. displacement plot of the strip footing with varying cohesion of the soil that with increase in the value of cohesion, the ultimate capacity (i.e., ultimate load) of the strip footing is increased. Similarly, the effect of friction angle of the soil on the ultimate capacity of the strip footing is depicted in Fig. 3b. It is observed from the load vs. displacement plot of the strip footing with varying friction angle of the soil that with increase in the value of friction angle of the soil, the ultimate capacity of the strip footing is increased. The effect of dilatancy is accounted by using a hypothetical dilatancy angle, $\psi = 15°$ for the case of friction angle, $\phi' = 15°$. The load vs. displacement plot of the strip footing corresponding to $\phi' = 15°$ and $\psi = 15°$ is also plotted in Fig. 3b. From the results, it is observed that the ultimate load of the strip footing is directly proportional to the strength parameters (c', ϕ', and ψ). This observation of increase in ultimate load with increase in the strength parameters of soil can be revealed from the classical solution of Terzaghi [26] for the strip footing. It is noted that the computation time required to reach the ultimate load corresponding to 50 mm displacement in the present case is lesser for lower values of c' and ϕ'.

Effect of width of footing, unit weight of soil and surcharge

The effect of width of footing on the ultimate capacity of the strip footing is depicted in Fig. 4a. It is seen from the figure that with increase in the width of the footing the ultimate load is increased. The mobilization of shear strength is over the larger zone and hence the increase in the ultimate capacity. Similarly, the effect of varying unit weight of the soil on the ultimate capacity of the strip footing is depicted in Fig. 4b. It is observed from the figure that with increase in the unit weight of the soil, the ultimate load is increased. Finally, the effect of surcharge on the ultimate capacity of the strip footing is depicted in Fig. 4c. It is seen from the figure that with increase in the magnitude of surcharge, the ultimate load of the strip footing is increased. The observations of increase in ultimate load with increase in the width of the footing, unit weight of the soil and magnitude of surcharge can be revealed from the classical solution of Terzaghi [26] for the strip footing. It is noted that the computation time required to reach the ultimate load corresponding to 50 mm displacement in the present case is lesser for lower values of B, γ, and q.

Effect of deformation parameters

Figure 5a, b depicts the load vs. displacement plots of the strip footing with varying deformation parameters of the soil as $E = 50$, 100, and 200 MPa and $\nu = 0.15$, 0.25, 0.35, and 0.45. It is observed from the figures that the varying deformation parameters will not have any effect on the ultimate load of the footing. It can be stated that the ultimate load is reached at lesser displacement when the higher values are assigned to the Young's modulus (twofold higher than the actual value) and Poisson's ratio (likely range 0.35–0.45). Based on the present study, if the aim of the FE analysis is to determine the failure load, the higher values of E and ν should be assigned to obtain the failure load at lesser displacement. It is also noted that the computation time required to reach the ultimate load corresponding to 50 mm

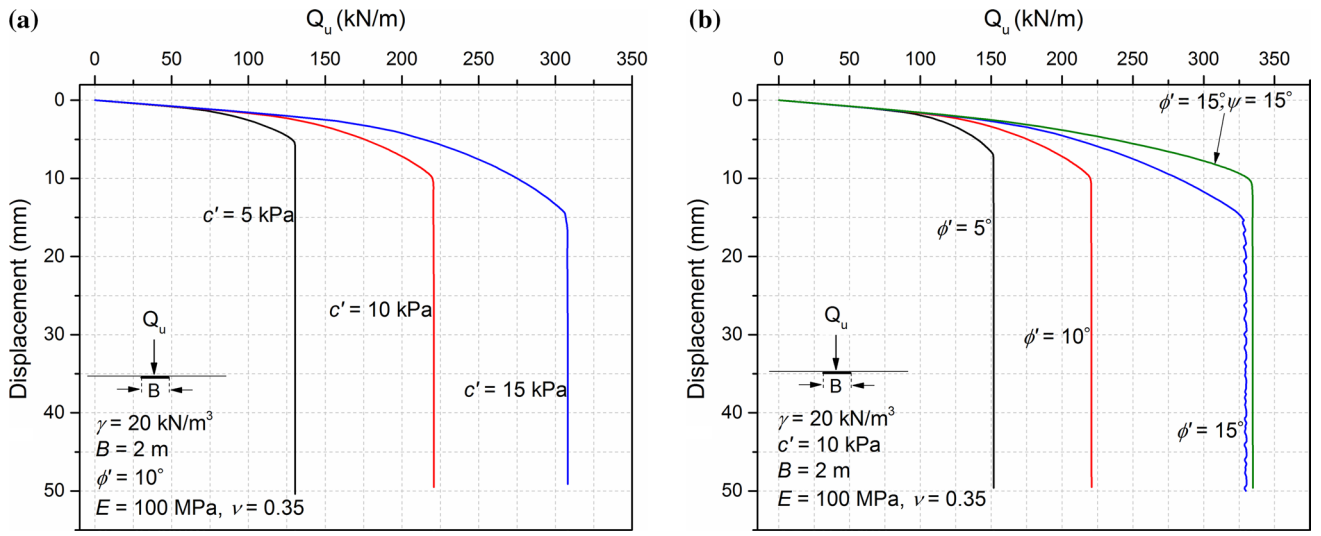

Fig. 3 Load vs. displacement plot of strip footing with varying: **a** cohesion, **b** friction angle of soil and a specific value of dilatancy angle $\psi = 15°$

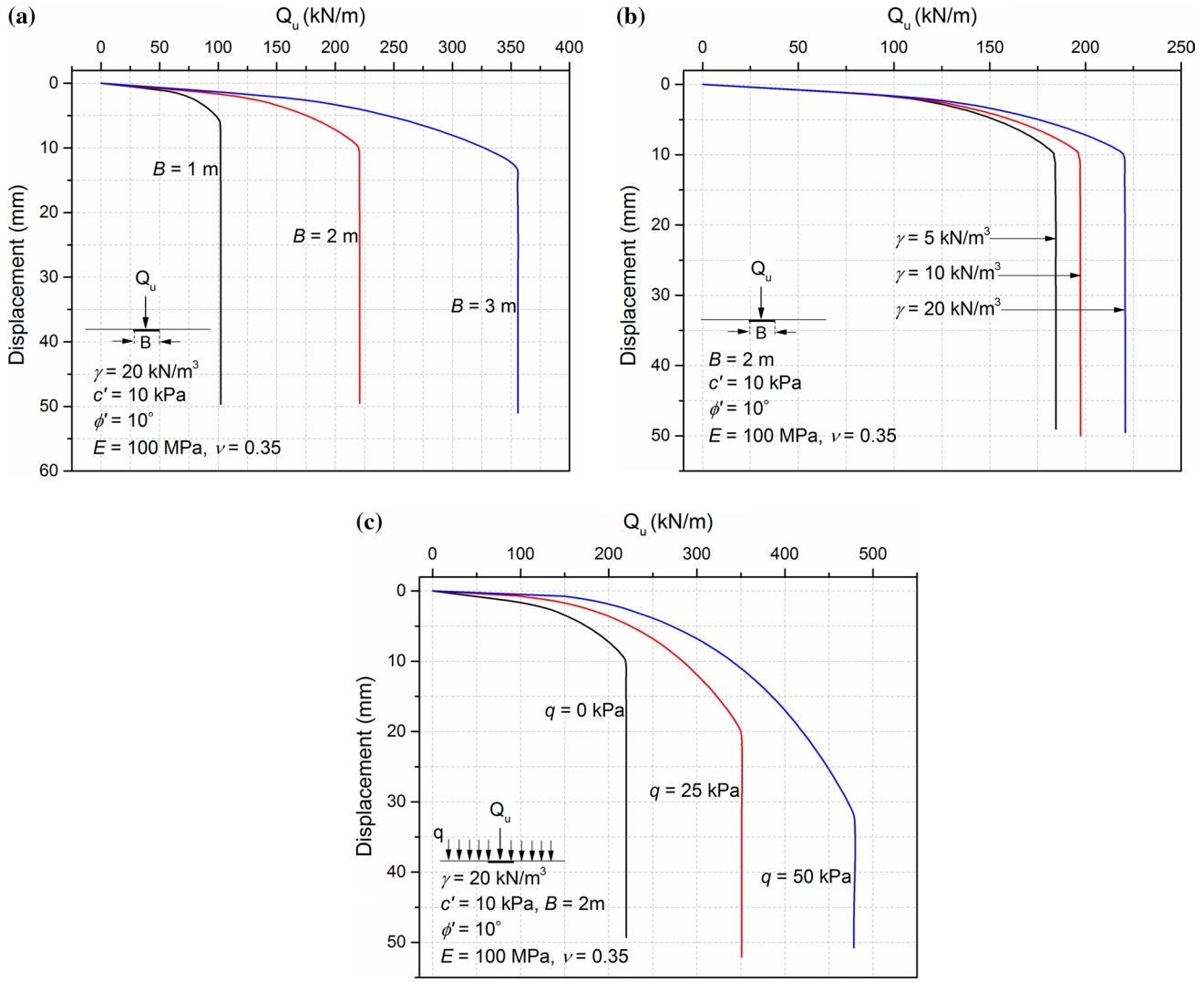

Fig. 4 Load vs. displacement plot of strip footing with varying: **a** footing width, **b** unit weight of soil, **c** surcharge

displacement is same irrespective of the different values of E and ν used in the analysis.

Effect of material model

The failure load corresponding to MC, HS, HSsmall, and SS model is determined from the load vs. displacement plot of the rough strip footing of width 2 m resting on soil having unit weight, $\gamma = 20$ kN/m^3 and strength parameters, $c' = 10$ kPa, $\phi' = 10°$, and $\psi = 0°$. Figure 6 depicts the load vs. displacement plot of the strip footing corresponding to each of the material models used in the analysis. All the material models use the strength parameters as defined by the Mohr–Coulomb failure envelope. Based on the results, it is observed that the ultimate failure loads obtained are almost the same corresponding to the four material models used in the FE analysis. It is attributed to the fact that in all these models, the limiting state of stress is described using the soil cohesion, the friction and dilatancy angles of the soil as used in the Mohr–Coulomb model. It is to be noted that the HS, HSsmall, and SS models have yielding cap to close the elastic region for the compressive stress paths. The computation time and the number of iterations required to reach the ultimate state of stress is less in the case of Mohr–Coulomb model compared to the HS, HSsmall, and SS models. In order to verify this finding, the FE analysis of the triaxial test is carried out with the same input parameters as used in the material models of the strip footing. The plots of deviator stress vs. axial strain and stress path are extracted to evaluate the independency of the material models. The FE results of the triaxial tests are discussed in "Triaxial test".

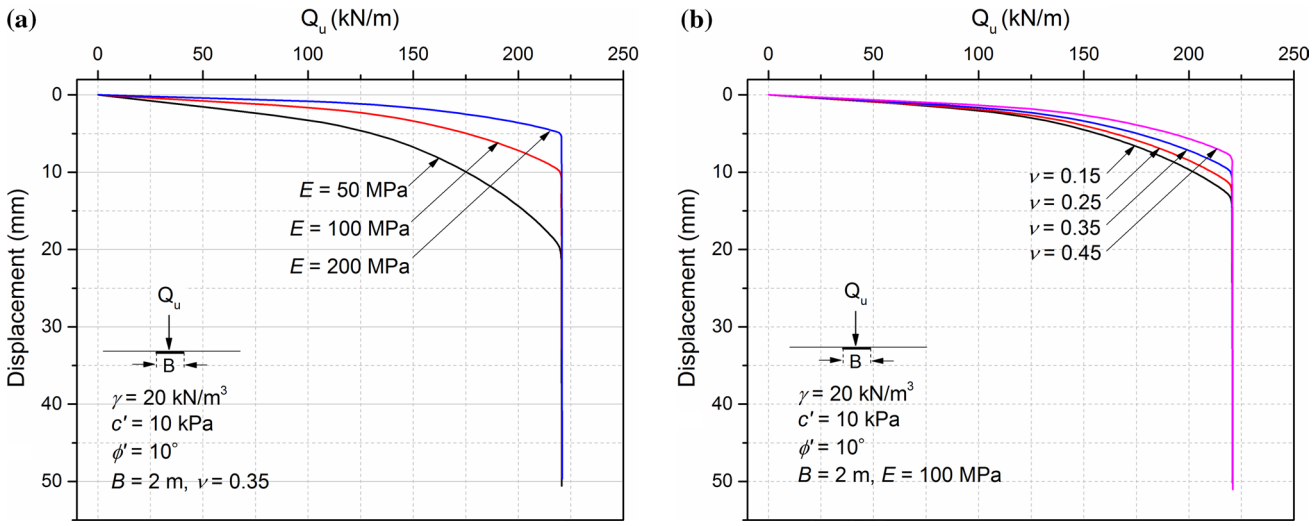

Fig. 5 Load vs. displacement plot of strip footing with varying: **a** Young's modulus, **b** Poisson's ratio

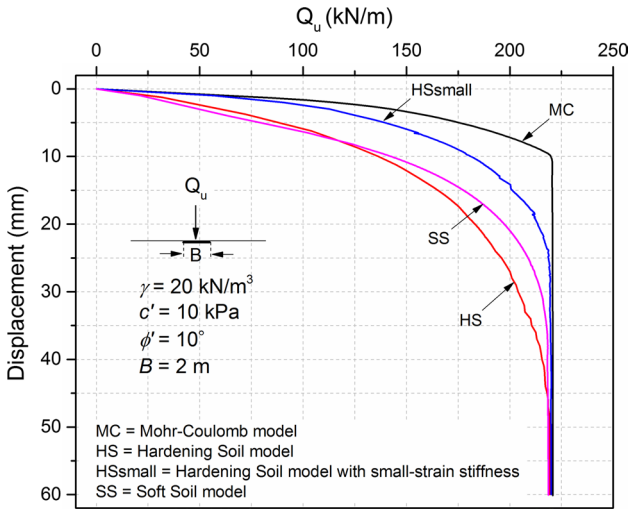

Fig. 6 Load vs. displacement plot of strip footing with different material models

Comparison of FE results and analytical solution

The ultimate loads obtained from the FE analyses corresponding to the varying parameters (B, c', ϕ', γ, and q) are compared with the analytical solutions of Terzaghi [26] and Meyerhof [19] (Table 2). After carefully going through the reported values of bearing capacity factors in the literature, it is found that these analytical solutions can be taken as upper and lower bound solutions for the strip footing, respectively. The deviation of FE results from Terzaghi [26] and Meyerhof [19] in percentage is also given in Table 2. From Table 2, it is observed that the ultimate load obtained from the FE analysis lies in between the solutions of Terzaghi and Meyerhof. The FE results are higher by 7–26% with respect to Meyerhof's solution and lesser by 5–11% with respect to Terzaghi's solution. The bearing capacity factors evaluated using the FEM are also found to be lesser than the upper bound values of Terzaghi [26] as reported by Griffiths [9]. It can be stated that the bearing capacity factors of the strip footing, N_c, N_q, and N_γ, can be computed fairly accurate using the FEM and they will lie in between the solutions of Terzaghi and Meyerhof.

Triaxial test

In order to verify the independency of the material models used in the present study (MC, HS, HSsmall, and SS) on the ultimate load of the strip footing, the FE model of the drained triaxial test is analyzed using PLAXIS program. The advantage of symmetry is taken and only one-fourth of the triaxial specimen is modeled. The model dimensions and boundary conditions are depicted in Fig. 7. The confining pressure (σ_3) is simulated using line load function, which is varied as 50, 100 and 150 kPa. The prescribed displacement of 10 mm is assigned at the top boundary of the model and for computing the failure stress at Gauss point B, which is selected within the FE mesh as shown in Fig. 7. The input parameters corresponding to each of these material models are same as in Table 1. The deviator stress (σ_1–σ_3) vs. ε_1 is plotted corresponding to the confining pressures of 50, 100 and 150 kPa for all the material models (Fig. 8a). It can be seen from the figure that $|\sigma_1$–$\sigma_3|$ reaches to the same maximum value as the axial strain (ε_1) increases for all the material models. In the case of $|\sigma_1$–$\sigma_3|$ vs. ε_1 plot for SS model, the initial displacement in the figure (Fig. 8a) is corresponding to the confining pressure applied. The stress path is also plotted from the FE results. Figure 8b

Table 2 Comparison of FE results with Terzaghi [26] and Meyerhof [19] results

Parameters	Ultimate load causing failure (kN)			Deviation of FEM results (%) from	
	Present study (FEM)	Terzaghi [26]	Meyerhof [19]	Terzaghi [26]	Meyerhof [19]
$B = 1$ m	102.197	108	87.4	− 5.37	+ 16.93
$B = 2$ m	220.8	240	183	− 8.00	+ 20.66
$B = 3$ m	355.974	396	286	− 10.11	+ 24.47
$c' = 5$ kPa	130.5	144	99.4	− 9.38	+ 31.29
$c' = 10$ kPa	220.8	240	183	− 8.00	+ 20.66
$c' = 15$ kPa	308.076	336	266	− 8.31	+ 15.82
$\phi' = 5°$	151.72	166	134	− 8.60	+ 13.22
$\phi' = 10°$	220.8	240	183	− 8.00	+ 20.66
$\phi' = 15°$	329.81	358	263	− 7.87	+ 25.40
$\gamma = 5$ kN/m^3	184.54	204	171	− 9.54	+ 7.92
$\gamma = 10$ kN/m^3	197.38	216	175	− 8.62	+ 12.79
$\gamma = 20$ kN/m^3	220.8	240	183	− 8.00	+ 20.66
$q = 0$	220.8	240	183	− 8.00	+ 20.66
$q = 25$ kPa	350.93	375	308	− 6.42	+ 13.94
$q = 50$ kPa	478.08	510	433	− 6.26	+ 10.41

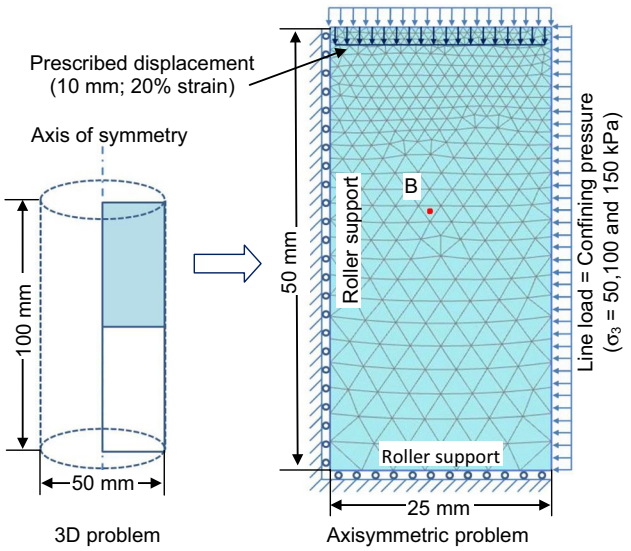

Fig. 7 Simplified geometry of triaxial test and FE mesh with boundary conditions

depicts the stress path corresponding to the MC, HS, HSsmall, and SS models. It is seen from the figure that the failure stress attains the same value for all the material models and touched the failure plane.

Conclusions

In this study, the FE analysis is carried out using PLAXIS program and the ultimate failure load of the strip footing resting on c-ϕ soil is computed. The sensitivity analysis is carried out and the effect of variation in strength parameters, deformation parameters, unit weight of soil, surcharge at the base level of the footing, and the width of the footing on the ultimate failure load is examined. The effect of material models like Mohr–Coulomb (MC) model, Hardening Soil (HS) model, Hardening Soil model with small-strain stiffness (HSsmall), and Soft Soil (SS) model on the ultimate failure load of the strip footing is also examined. The FE results are compared with the analytical solutions of Terzaghi [26] and Meyerhof [19]. Based on the study, the following conclusions are arrived at:

1. The ultimate failure load obtained from the FE analysis increases with the increase in the strength parameters of the soil, unit weight of the soil, width of the footing, and the magnitude of the surcharge at the base of footing.
2. At higher values of the Young's modulus and Poisson's ratio, the ultimate failure load of strip footing is reached at the smaller displacement. The ultimate failure load for the given soil will not change with the change in the deformation parameters of the soil.
3. The MC, HS, HSsmall, and SS models use the strength parameters as defined by Mohr–Coulomb failure envelope and they compute the same ultimate failure load for the strip footing. The FE simulations of the triaxial tests also verify the independency of the material mod-

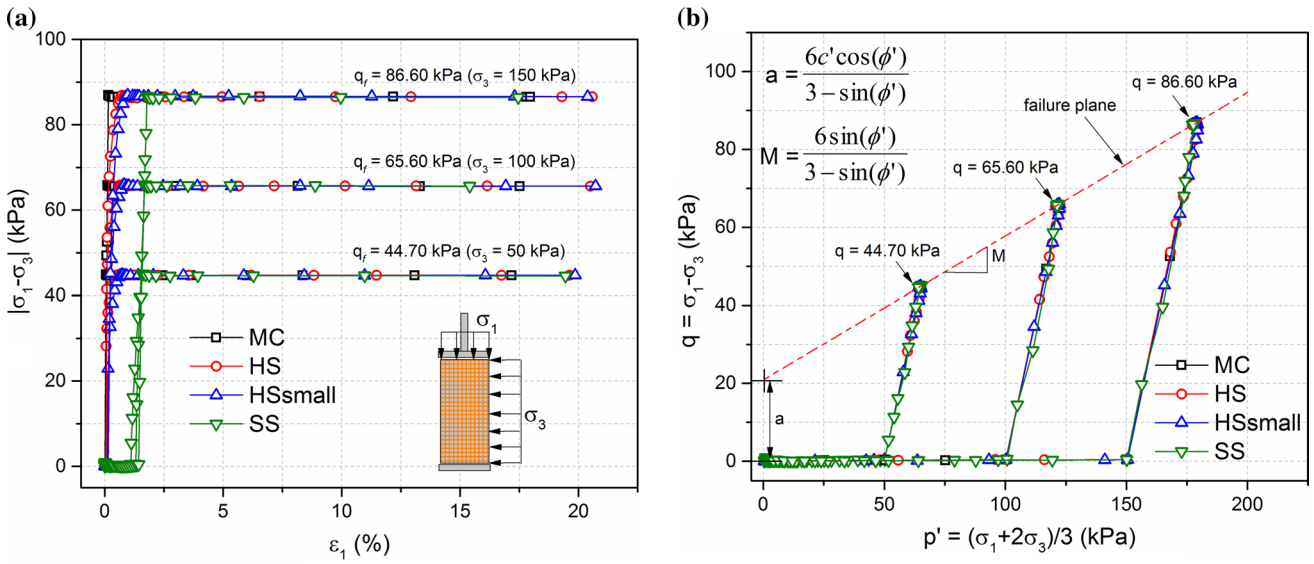

Fig. 8 Drained triaxial test results for different material models: **a** $|\sigma_1-\sigma_3|$ vs. ε_1, **b** stress path

els used in this study by computing the same failure stresses. The computation time to reach the ultimate state of stress is more for the HS, HSsmall, and SS models as compared to the MC model.

4. The comparison of FE results of the strip footing with the analytical solutions of Terzaghi and Meyerhof gave confidence in using the FE analysis for stability analysis of geomechanics problems.

Recommendations

If the objective of the analysis is to evaluate only the collapse load, it is recommended to use the Mohr–Coulomb material model in lieu of the other constitutive models used in this study. For the Mohr–Coulomb model, the computation time and number of iterations needed to obtain the ultimate load are less in comparison to the other models like Hardening Soil model, Hardening Soil model with small-strain stiffness, and Soft Soil model. A number of input parameters used in the Mohr–Coulomb model are also less in comparison to the other models. In order to obtain the quick results for the determination of collapse load using the Mohr–Coulomb model in FE analysis, one has to assign the higher values to the Young's modulus and Poisson's ratio. It is to be noted that the ultimate failure load of the strip footing is independent of the deformation parameters and reached its ultimate value at a lesser displacement if the higher values of Young's modulus (twofold higher than the actual value) and Poisson's ratio (likely range 0.35–0.45) are assigned.

Appendix 1

Mohr–Coulomb model In Mohr–Coulomb (MC) model, the yield function consists of principal stresses and strength parameters of the soil, c' and ϕ' [2]. In the principal stress space, the Mohr–Coulomb failure envelope represents a straight line at the intersection with an octahedral plane. It is shown to provide a good fit to the experimental data in triaxial compression and extension. The Mohr–Coulomb material model can be used most conveniently in the numerical simulation. The defining parameters are: the unit weight of soil, strength parameters (c', ϕ', and ψ), deformation parameters (E and ν), and K_0 is coefficient of earth pressure at rest which is by default taken as 1 – sin (ϕ').

Hardening Soil model The Hardening Soil (HS) model is an advanced soil model which is an isotropic hardening double surface plasticity model, in which the stiffness is described based on three input stiffness. They are the triaxial loading stiffness (E_{50}), the triaxial unloading stiffness (E_{ur}), and the oedometer loading stiffness (E_{oed}), which account for the stress dependency of the stiffness values. The HS model [23] gives more realistic displacement patterns for the working load conditions, especially in the case of an excavation. The input parameters of HS model are: the unit weight of soil (γ), soil cohesion (c'), friction and dilatancy angles of soil (ϕ' and ψ), triaxial loading stiffness (E_{50}), triaxial unloading stiffness (E_{ur}), oedometer loading stiffness (E_{oed}), Poisson's ratio (ν), power for stress level dependency of stiffness (m), K_0^{nc} for normal consolidation, and failure ratio (R_f).

Hardening Soil model with small-strain stiffness The Hardening Soil model with small-strain stiffness is a modification of the Hardening Soil model that accounts for the

increased stiffness of the soil at small strains. This model is most apparent in working load conditions and gives more reliable displacements than the HS model. It has the same defining parameters of HS model with two additional parameters, i.e., small-strain shear modulus (G_0) and the shear strain level ($\gamma_{0.7}$) at which the shear modulus has reduced to about 70% of the G_0.

Soft Soil model The Soft Soil (SS) model is a Cam-clay type model especially meant for the primary compression of near normally consolidated clay type soils, which is better in capturing the compression of very soft soils. The input parameters of SS model are: the unit weight of soil (γ), soil cohesion (c'), friction and dilatancy angles of soil (ϕ' and ψ), modified compression index (λ^*), modified swelling index (κ^*), Poisson's ratio (ν), and K_0^{nc} for normal consolidation.

References

1. Bolton MD, Lau CK (1993) Vertical bearing capacity factors for circular and strip footings on Mohr–Coulomb soil. Can Geotech J 30(6):1024–1033
2. Brinkgreve RBJ, Vermeer PA, Bakker KJ (1988) Material model manual, PLAXIS V.7, A.A. Balkema, Rotterdam, Brookfield
3. Chakraborty D (2016) Bearing capacity of strip footings by incorporating a non-associated flow rule in lower bound limit analysis. Int J Geotech Eng 10(3):311–315
4. Chandrashekhara K, Antony SJ, Mondal D (1998) Semi-analytical finite element analysis of a strip footing on an elastic reinforced soil. Appl Math Model 22(4–5):331–349
5. Chen WF (1975) Limit analysis and soil plasticity. Elsevier, Amsterdam
6. Drucker DC, Greenberg HJ, Prager W (1951) The safety factor of an elastic–plastic body in plane strain. J Appl Mech ASME 18:371–378
7. Drucker DC, Prager W, Greenberg HJ (1952) Extended limit design theorems for continuous media. Q Appl Math 9(4):381–389
8. Frydman S, Burd HJ (1997) Numerical studies of the bearing capacity factor N_γ. J Geotech Eng 123(1):20–29
9. Griffiths DV (1982) Computation of bearing capacity factors using finite elements. Géotechnique 32(3):195–202
10. Griffiths DV (1989) Computation of collapse loads in geomechanics by finite elements. Arch Appl Math 59(3):237–244
11. Hansen JB (1961) A general formula for bearing capacity. B Geoteknisk Institut, B 11, The Danish Geotech Inst, Copenhagen
12. Hjiaj M, Lyamin AV, Sloan SW (2004) Bearing capacity of a cohesive-frictional soil under non-eccentric inclined loading. Comput Geotech 31(6):491–516
13. Kumar J (2004) Effect of footing—soil interface friction on bearing capacity factor N_γ. Géotechnique 54(10):677–680
14. Kumar J (2009) The variation of N_γ with footing roughness using the method of characteristics. Int J Num Anal Methods Geomech 33(2):275–284
15. Kumar J, Khatri V (2008) Effect of footing roughness on lower bound N_γ values. Int J Geomech ASCE 8(3):176–187
16. Kumar J, Kouzer KM (2007) Effect of footing roughness on bearing capacity factor N_γ. J Geotech Geoenviron Eng ASCE 133(5):502–511
17. Maheshwari P, Madhav MR (2006) Analysis of a rigid footing lying on three-layered soil using the finite difference method. Geotech Geol Eng 24(4):851–869
18. Meyerhof GG (1957) The ultimate bearing capacity of foundations on slopes. In: proc 4th int conf soil mech found eng, London, 1: 384–386
19. Meyerhof GG (1963) Some recent research on the bearing capacity of foundations. Can Geotech J 1(1):16–26
20. Michalowski RL (1997) An estimate of the influence of soil weight on bearing capacity using limit analysis. Soils Found 37(4):57–64
21. Murray EJ, Geddes JD (1989) Resistance of passive inclined anchors in cohesionless medium. Geotechnique 39(3):417–431
22. Sahoo JP, Kumar J (2015) Ultimate bearing capacity of shallow strip and circular foundations by using limit analysis, finite elements, and optimization. Int J Geotech Eng 9(1):30–41
23. Schanz T, Vermeer PA, Bonnier PG (1999) The hardening-soil model: formulation and verification. In: Brinkgreve RBJ (ed) Beyond 2000 in computational geotechnics. Balkema, Rotterdam, pp 281–296
24. Sloan SW (1988) Lower bound limit analysis using finite-elements and linear programming. Int J Num Anal Methods Geomech 12(1):61–77
25. Soubra AH (1999) Upper-bound solutions for bearing capacity of foundations. J Geotech Geoenviron Eng ASCE 125(1):59–68
26. Terzaghi K (1943) Theoretical soil mechanics. Wiley, New York
27. Ukritchon B, Whittle AJ, Klangvijit C (2003) Calculation of bearing capacity factor N_γ using numerical limit analyses. J Geotech Geoenviron Eng ASCE 129(5):468–474
28. Veiskarami M, Kumar J, Valikhah F (2014) Effect of the flow rule on the bearing capacity of strip foundations on sand by the upper-bound limit analysis and slip lines. Int J Geomech ASCE 14(3):04014008
29. Yin J, Wang Y, Selvadurai A (2001) Influence of nonassociativity on the bearing capacity of a strip footing. J Geotech Geoenviron Eng ASCE 127(11):985–989
30. Ziccarelli M, Valore C, Muscolino SR, Fioravante V (2017) Centrifuge tests on strip footings on sand with a weak layer. Geotech Res 4(1):47–64
31. Zienkiewicz OC, Humpheson C, Lewis RW (1975) Associated and nonassociated visco-plasticity and plasticity in soil mechanics. Géotechnique 25(4):671–689